A Thesis of Master's Degree

Assessment of Early Therapeutics Response to Nitroxoline in Temozolomide Resistant Glioblastoma by Amide Proton Transfer Imaging: Comparison with Diffusion-weighted Imaging

February 2019

Interdisciplinary Program in Cancer Biology Major

Graduate School

Seoul National University

Nishant Thakur

※ 석사학위논문 내표지(인준지)

Assessment of Early Therapeutics Response to Nitroxoline in Temozolomide Resistant Glioblastoma by Amide Proton Transfer Imaging: Comparison with Diffusion-weighted Imaging

지도교수 최승홍

이 논문을 **Nishant Thakur** 석사학위논문으로 제출함

2018 년 10 월

서울대학교 대학원

협동과정 종양생물학 전공

Nishant Thakur

Nishant Thakur 석사학위논문을 인준함

2018 년 12월

위 원 장 _____ (인)

부 위 원 장 _____ (인)

위 원 _____ (인)

Abstract

Assessment of Early Therapeutic Response to Nitroxoline in Temozolomide-Resistant Glioblastoma by Amide Proton Transfer Imaging: Comparison with Diffusion-weighted Imaging

Interdisciplinary Program in Cancer Biology Major
Graduate School
Seoul National University

Purpose: Amide proton transfer (APT) imaging is a novel molecular MRI technique to detect endogenous mobile proteins and peptides through chemical exchange saturation transfer. The purpose of this study was to evaluate the feasibility of amide proton transfer (APT) imaging in monitoring the early therapeutic response to nitroxoline (NTX) in temozolomide (TMZ)-resistant glioblastoma multiforme (GBM) mouse model, which was compared with diffusionweighted imaging (DWI).

Methods: This study was approved by the institutional animal care and use committee of Seoul National University Hospital. Here, we prepared TMZ-resistant GBM mouse model (n = 12), which were treated with 100mg/kg/d of NTX (n = 4) or TMZ (n = 4), or saline (n = 4) for 7 days for the evaluation of short-term treatment by using APT imaging and DWI sequentially. The APT signal intensities and apparent diffusion coefficient (ADC) values were calculated and compared before and after treatment. The immunohistological analysis was also employed for the correlation between APT imaging and histopathology. The association between the APT value and Ki67 labeling index were evaluated by

using simple linear regression analysis.

Results: We observed that the tumor volume decreased without significance after short-term NTX therapy (P = 0.6857), while tumor volume increased without significance in control (P = 0.2000) and TMZ groups (P = 0.1143). Furthermore, the short-term NTX treatment (P = 0.0286) resulted in significant decrease in APT value as compared to untreated (P = 0.3429) and TMZ group (P = 0.1143), in which APT signals were increased. However, we did not observe significantly increased mean ADC value following short-term NTX treatment (P = 0.2000). In contrast, the mean ADC value was significantly decreased in untreated (P = 0.0286) as well as TMZ-treated mice (P = 0.0286). In addition, our histological data showed that, the expression of Ki67, which was significantly lower in the NTX-treated group than in the untreated and TMZ group. Moreover, the Ki67 labeling index shows a correlation with APT value.

Conclusion: APT imaging could show the earlier response to NTX treatment as compared to ADC values in a TMZ-resistance, mouse model. We believe that APT imaging can be a useful imaging biomarker for the early therapeutic evaluation in GBM patients.

……

Keywords: Amide proton imaging, apparent diffusion coefficient, chemical exchange saturation transfer imaging, nitroxoline, temozolomide-resistant glioblastoma.

***Student Number*: 2016-24265**

Index

1. Introduction
2. Materials and Methods
    2-1. Study design
    2-2. MR imaging protocol and analysis
    2-3. Histology analysis
    2-4. Statistical Analysis
3. Results
    3-1. Comparison of early evaluation of NTX-mediated therapeutic effects by APT and ADC
    3-2. Quantification of immunohistochemistry studies
4. Discussion
5. References
6. Figures
7. Korean Abstract

Introduction

Glioblastoma multiforme (GBM) is the most malignant primary brain tumor in adults and is uniformly fatal. The current standard of care for glioblastoma includes safe surgical resection, radiotherapy, and temozolomide (TMZ) treatment [1,2]. The development of resistance to radiotherapy and TMZ is common [3,4] and the heterogeneous nature of glioblastoma further complicates these therapies [5]. Unfortunately, average survival is still less than two years [1]. Surveillance of the tumor response to drug treatment is essential for treatment supervision or to make any decision [6]. Magnetic resonance imaging (MRI) is a standard neuroimaging technique currently used in the clinical evaluation of the response to therapy based on the detection of tumor size [7]. However, subsidiary imaging methods that can determine the drug response and scrutinize drug-target engagement are critically needed to improve opportune clinical patient management.

One attainable approach is the imaging of metabolism. Altered metabolism has been considered a hallmark of cancer and has been recognized as an important mechanism and biomarker for cancer [8]. There are significant alterations in the metabolic profile between healthy and diseased brain tissue that can be detected in patients by using MRI. However, monitoring the response to therapies can be challenging because tumor shrinkage is not always observed [9]. Advanced MR techniques such as diffusion-weighted MRI (DWI), perfusion MRI, and 1H magnetic resonance spectroscopy (MRS) have also been used to monitor brain tumor response to therapy [10-12], but it may take several weeks to detect a response to therapy. Therefore, it is imperative to develop novel imaging modality that can easily characterize the progressive tumor and the early therapeutic effect that would help to decide for ineffective and respondent treatment. Proteins perform many

cellular activities, and various lesions, such as those found in tumors, may show changes in the concentration and properties of proteins and peptides [13]. Therefore, information at the protein level may be relevant for earlier detection, better spatial definition, and improved characterization of diseases [14,15]. Amide proton transfer (APT) imaging, one subset of chemical exchange saturation transfer (CEST) imaging, has been introduced as a potentially useful technique that reflects cellular protein and the physical and chemical properties of tissue with image contrast provided by using endogenous mobile proteins or peptides and information on the pH of the tissue [16-18] that is not available via conventional MRI measures. In addition, APT asymmetry values have been proposed as prognostic indicators of brain glioma, as they reflect the cellular proliferation levels that correlate with Ki67 [19], and as sensitive biomarkers of treatment response in experimental and clinical studies [20].

Nitroxoline (NTX) is an FDA approved antibiotic repurposed for cancer. Lezovic et.al revealed that NTX induces apoptosis and slows glioma growth *in vivo*, resulting in a significantly increased ADC value in a PTEN/KRAS glioma model as determined by DWI following NTX treatment (80 mg/kg/day) for 14 days [21]. We speculated about other imaging modalities with the ability to assess early therapeutic effects of drugs that may help to determine whether the treatment is effective and should be continued or not. The purpose of this study was to evaluate the feasibility of APT imaging in monitoring the early therapeutic response to NTX in a TMZ-resistant GBM mouse model, which was compared with DWI. We also correlated APT imaging parameters with histopathological findings.

Materials and Methods

Study design

Figure 1 summarizes the *in vivo* experiments. The animal experiments were approved by the Institutional Animal Care and Use Committee of Seoul National University Hospital. To prepare for the orthotopic GBM mouse model, 6-week-old male BALB/c nude mice (n = 12, 4 in each group) were anesthetized using intraperitoneal injection of a mixture of Zoletil (Zolazepam) and Rompun (Xylazine) and were placed in a stereotaxic device. The mice were inoculated with LN229 (ATCC, CRL-2611) human glioma cells ($3x10^6$ cells). The cells were injected in the caudate/putamen region of the brain by using a Hamilton syringe fitted with a 28-gauge needle, which was positioned with a syringe attachment fitted to the stereotaxic device. Pretreatment T2WI confirmed the required tumors 2 weeks after tumor implantation. TMZ-resistance models were developed by subjecting mice with GBM to successively high doses of TMZ (100 mg/kg/day) until tumor growth showed no inhibition by TMZ for 7 days, as described in previous studies [3,31,32]. The models were further confirmed by T2WI, referred to as the post-1 MRI. The animals were intraperitoneally treated with 100 mg/kg/day of NTX or saline for 7 days in the NTX and control groups, respectively. In the TMZ group, the animals were treated with 100 mg/kg/day of TMZ for 7 days after post 1 MRI. The post-2 MRI was conducted after drug treatment to evaluate the therapeutic effects on tumor growth. APT imaging and DWI were also acquired sequentially with T2WI in pretreatment, post-1, and post-2 MRIs.

MR imaging protocol and analysis

For the *in vivo* animal MRI, animals were anesthetized with 1.5–2% isoflurane/oxygen (v/v), and then scanned using a 9.4T MR scanner (Agilent Technologies, Santa Clara, CA, USA). Throughout each imaging session, the animals were wrapped in warm water blankets, and their oxygen saturation and heart rates were monitored. In anatomic T2WI in the coronal plane, fast spin-echo multiple slices were employed with the following parameters: [TR = 3000 ms, effective TE = 31.18 ms, ETL = 4, averages = 2, data matrix size = 256 x 256, and field of view (FOV) = 25.0 x 25.0 mm^2]. APT imaging with coronal plane was performed by using a prototype 2-dimensional saturation pulse target frequency 3.5 ppm, saturation pulse duration 5 s, slice thickness 1.00 mm, saturation pulse power 20 Hz followed by four-shot, spin-echo, echo-planar imaging acquisition [TR = 5500 ms, TE = 9.34 ms, ETL = 4, averages = 1, data matrix = 128 x 128, field of view (FOV) = 25.0 x 25.0 mm^2]. The echo-planar DWI with coronal plane was obtained as followings: [TR = 4000 ms, TE = 60.04 ms with shots 2, repetitions = 1, average = 2, data matrix = 128 x 128, field of view (FOV) = 24.0 x 24.0 mm^2, b-value = 0, 100, 200, 400, 700 and 1000 s/mm^2, and slice thickness = 1 mm]. The APT and ADC maps were generated, and image analysis was performed by using our in-house software developed with a commercial analysis package (Matlab version R2007b, MathWorks Inc., Natick, MA, USA).

The Author was blinded to the experimental data drew regions of interest (ROIs) that contained the entire tumor on every continuous section of the coregistered T2WI, APT and ADC maps. Tumor boundaries were defined regarding the high signal intensity on T2WI. Then, we calculated tumor volume, and mean APT and ADC values from each tumor.

Histology analysis

At the end of the post-2 MRI studies, all animals were sacrificed and perfused with normal saline, and brains were harvested for histological analysis. All coronal sections were stained with hematoxylin and eosin (H&E) for tumor morphology. For immunohistochemical analysis, the primary antibody and their dilutions were as follows: mouse monoclonal antibody to Ki67 (1:200; no. UM 8033; UltraMab) was used for 1 hour at room temperature. Then, the sections were rinsed with washing buffer and incubated with horseradish peroxidase-conjugated secondary antibodies (Santa Cruz Biotechnology) for 30 minutes at room temperature. Staining for the detection of bound antibodies was evaluated by DAB. Ki67-positive cells and TUNEL-positive cells were calculated by ImageJ software. Additionally, brain tumor sections were subjected to TUNEL assay to measure apoptotic tumor cells.

Statistical Analysis

All statistical analyses were performed using a commercial software program (MedCalc version 13.1.0.0, MedCalc Software). A P value of < 0.05 was considered statistically significant. Kolmogorov-Smirnov's test was used to determine whether the noncategorical variables were normally distributed. Nonparametric data are presented as the median and interquartile range (IQR, range from the 25th to the 75th percentile), and parametric data are shown as the mean ± standard deviation. According to the results of the Kolmogorov-Smirnov's test, paired or unpaired Student's t-test, Wilcoxon test or Mann-Whitney U-test was performed where appropriate to compare the values between the two groups. The

Kruskal-Wallis test calculated the comparison between the three experimental groups. The association between the APT value and Ki67 labeling index was evaluated by using simple linear regression analysis.

Results

Comparison of early evaluation of NTX-mediated therapeutic effects by APT and ADC

Figure 2A shows representative T2WI, APT, and ADC maps obtained in mice with TMZ-resistant GBM in control, NTX and TMZ-treated groups prior to and after treatment. We observed that the tumor volume decreased without significance in post-2 MRI compared to that in post-1 after short-term NTX therapy (6.26 [IQR, 5.31-8.04] vs 6.08 [IQR, 4.67-7.85]; P = 0.6857), while tumor volume increased without significance in post-2 MRI compared to that in post-1 in the control (3.73 [IQR, 3.39-5.24] vs 5.01 [IQR, 4.69-6.27]; P = 0.2000) and TMZ groups (6.02 [IQR, 5.17-6.87] vs 7.79 [IQR, 7.07-8.76]; P = 0.1143) (Fig. 2B). In terms of DWI, we did not observe a significantly increased mean ADC value (showed in x 10^{-3} mm^2/sec) in post-2 MRI following short-term NTX treatment (7.91 [IQR, 7.07-8.15] vs 8.79 [IQR, 7.61-9.23]; P = 0.2000). In contrast, the mean ADC value was significantly decreased on post-2 MRI in untreated (7.97 [IQR, 7.80-8.29] vs 7.29 [IQR, 7.14-7.35]; P = 0.0286) as well as TMZ-treated mice (8.71 [IQR, 8.54-8.72] vs 8.03 [IQR, 7.80-8.25]; P = 0.0286) (Fig. 2C). Interestingly, the significantly decreased APT values were observed in post-2 MRI in NTX-treated mice (2.74 [IQR, 2.29-3.34] vs 0.59 [IQR, 0.50-0.85]; P = 0.0286). The APT value was increased in post-2 MRI compared to that in post-1 in untreated mice (2.31 [IQR, 2.15-2.57] vs 2.88 [IQR, 2.37-3.80]; P = 0.3429) as well as in TMZ mice (1.49 [IQR, 1.16-2.11] vs 2.47 [IQR, 2.26-3.08]; P = 0.1143) (Fig. 2D). These results suggest that compared to ADC values, APT signals could provide better information on the early therapeutic response to chemotherapy.

Quantification of immunohistochemistry studies

Based on ours *in vivo* results, we performed immunohistology to identify the microscopic changes in tumors for the correlation between APT signals and histological findings. The histological examination of H&E, Ki67 and TUNEL stained brain sections from NTX-treated, TMZ-treated and untreated TMZ-resistant GBM bearing mice were used to confirm the morphology of tumors, proliferation, and apoptosis (Fig. 3A). The tumor proliferation index was evaluated by the protein expression of Ki67, which was significantly lower in the NTX-treated group than in untreated mice (control; 8.89 [IQR, 7.55-10.10] vs NTX; 5.14 [IQR, 4.63-5.75]; $P = 0.0209$). The level of cell proliferation was significantly increased following TMZ treatment compared to that following NTX treatment (TMZ; 7.98 [IQR, 6.46-9.38] vs NTX; 5.15 [IQR, 4.63-5.75]; $P = 0.0209$). There was no significant difference in cell proliferation between TMZ-treated and untreated animals (control; 8.89 [IQR, 7.55-10.10] vs TMZ; 7.98 [IQR, 6.46-9.38]; $P = 0.2482$) (Fig. 3B). Furthermore, the number of apoptotic cells was investigated by TUNEL assay staining in which a significantly increased number of apoptotic cells were observed following NTX treatment (control; 0.13 [IQR, 0.09-0.17] vs NTX; 0.30 [IQR, 0.21-0.41]; $P = 0.0209$) compared to that following the control. However, there was no significant difference of apoptosis between the untreated and TMZ-treated animals (control; 0.13 [IQR, 0.09-0.17] vs TMZ; 0.17 [IQR, 0.09-0.27]; $P = 0.5637$) or between the NTX- and TMZ-treated mice (NTX; 0.30 [IQR, 0.21-0.41] vs TMZ; 0.17 [IQR, 0.09-0.27]; $P = 0.2482$) (Fig. 3C). Furthermore, we observed that the Ki67 labeling index between all experimental groups showed a correlation with APT value ($R^2 = 0.536$, $P = 0.0068$) (Fig. 4).

Discussion

In the present study, we employed two techniques, APT imaging and DWI, to assess the early therapeutic effects of NTX in a TMZ-resistant GBM mouse model. APT and ADC values were analyzed. APT imaging (a subtype of CEST imaging, sensitive to amide protons resonating at 3.5 ppm from water) was designed to detect mobile (cytosolic) proteins and peptides [22]. Malignant gliomas are highly cellular and have a higher cellular content of proteins and peptides than healthy tissue, as revealed by MRI-guided proteomics and *in vivo* MR spectroscopy [23,24], and it has been assumed that amide proteins of endogenous mobile proteins and peptides in the cytoplasm are the major source of the APT signals [22]. In our study, we determined that APT imaging can detect metabolites that are elevated or down-modulated after NTX treatment. Short-term NTX treatment resulted in a substantial reduction in APT signals, although the tumor volume and ADC value did not detectably change by T2WI and DWI. The subsequent increase in APT value in the untreated group and TMZ-treated mice indicates the further progression of the tumor.

Generally, successful treatment may cause necrosis or apoptotic processes, leading to a reduction in cell density, which would increase the ADC values. Several studies have reported that the ADC is useful to estimate the aggressiveness of many cancers and correlates with progression-free survival [25,26]. However, in other reports, ADC was limited to malignancy evaluation, because a minimal change of ADC value cannot reflect the metabolic changes or changes in cellularity after early exposure to chemotherapeutic agents [27,28,29]. In our study, ADC value did not detectably change after NTX treatment by DWI. However, the ADC value was significantly decreased in the control and TMZ groups, which suggests increased

cellular proliferation in the tumor. The undetectable change in ADC value was not sufficient to evaluate the early response to NTX, while the APT value was dramatically decreased after NTX therapy. The undetectable change in mean tumor volume following short-term NTX treatment indicates that compared to no treatment and TMZ treatment, NTX slows down tumor growth. This result was similar to that of a previous study [21].

Although TMZ, a second-generation alkylating agent, is considered one of the best choices for standard adjuvant treatment for GBM, it is a DNA-damaging agent and induces apoptosis. One might assume that the 1-week exposure may be sufficient to induce APT changes in the NTX-treated group, which could be associated with apoptosis within the 7 days. To further scrutinize this possibility, we investigated the TMZ group in which we observed increased tumor volume and APT values after 2 weeks of TMZ treatment. Moreover, the change in ADC value was subsequently investigated in which we observed significantly decreased ADC values after TMZ treatment. This finding reflects further progression and the development of resistance to TMZ treatment.

Histological examination of the tissue showed that the 2-week TMZ treatment induced a marked increase in Ki67 expression, which results from increased mitosis. According to the relevant literature, the APT signals of brain tumors are positively correlated with cellular density and proliferation, arising from intracellular mobile proteins and peptide [19,30]. Similar to previous reports, we showed the positive correlation between APT signals and cellular proliferation as evaluated by Ki67 staining. This observation suggests that APT signals reflect the production of endogenous mobile proteins and peptides, which is associated with

tumor cell proliferation. Therefore, from this observation, we concluded that the decrease in APT values observed in NTX-treated mice reflects the proliferation arrest of tumor cells responding to chemotherapy well before the tumor volume and cellular density begins to decrease. As molecular changes occur early in the time course of chemotherapy, preceded by morphologic changes, which cannot be detected by conventional MRI; thus, APT signals may serve as an early biomarker of the degree of tumor progression or treatment response. Increased APT signals following TMZ treatment indicates the aggressiveness of recurrent GBM even after chemotherapy with TMZ. In relation to TMZ resistance, the enhanced tumor area increased drastically after 1 week of TMZ treatment compared to that at baseline, indicating that TMZ resistance was acquired as showed by the post-1 MRI. The results also demonstrate that APT signal does not decrease when the treatment is ineffective in case of TMZ-treated animals.

One limitation of this study should be mentioned. We included only four mice in all experimental groups. Our institutional policy is to minimize enrolled animal numbers; thus, we decided to conclude our study after observing statistical significance.

In summary, we concluded that compared to ADC values, APT imaging could show an earlier response to NTX treatment in a mouse TMZ-resistance model. APT imaging is a safe, completely noninvasive technology, and the results can be easily translated into the clinic. We believe that APT imaging can be a useful imaging biomarker for the early therapeutic evaluation in GBM patients.

References

1. Stupp, R. *et al.* Radiotherapy plus concomitant and adjuvant temozolomide for glioblastoma. *N Engl J Med* 352, 987-996, doi:10.1056/NEJMoa043330 (2005).
2. Sengupta, S., Marrinan, J., Frishman, C. & Sampath, P. Impact of temozolomide on immune response during malignant glioma chemotherapy. *Clin Dev Immunol* 2012, 831090, doi:10.1155/2012/831090 (2012).
3. Lee, S. Y. Temozolomide resistance in glioblastoma multiforme. *Genes & Diseases* 3, 198-210, doi:10.1016/j.gendis.2016.04.007 (2016).
4. Johannessen, T. C. & Bjerkvig, R. Molecular mechanisms of temozolomide resistance in glioblastoma multiforme. *Expert Rev Anticancer Ther* 12, 635-642, doi:10.1586/era.12.37 (2012).
5. Inda, M. M., Bonavia, R. & Seoane, J. Glioblastoma multiforme: a look inside its heterogeneous nature. *Cancers (Basel)* 6, 226-239, doi:10.3390/cancers6010226 (2014).
6. Macdonald, D. R., Cascino, T. L., Schold, S. C., Jr. & Cairncross, J. G. Response criteria for phase II studies of supratentorial malignant glioma. *J Clin Oncol* 8, 1277-1280, doi:10.1200/JCO.1990.8.7.1277 (1990).
7. Chinot, O. L. *et al.* Response assessment criteria for glioblastoma: practical adaptation and implementation in clinical trials of antiangiogenic therapy. *Curr Neurol Neurosci Rep* 13, 347, doi:10.1007/s11910-013-0347-2 (2013).
8. Pavlova, N. N. & Thompson, C. B. The Emerging Hallmarks of Cancer

Metabolism. *Cell Metab* 23, 27-47, doi:10.1016/j.cmet.2015.12.006 (2016).

9. Courtney, K. D., Corcoran, R. B. & Engelman, J. A. The PI3K Pathway As Drug Target in Human Cancer. *Journal of Clinical Oncology* 28, 1075-1083, doi:10.1200/Jco.2009.25.3641 (2010).

10. Tomura, N. *et al.* Diffusion changes in a tumor and peritumoral tissue after stereotactic irradiation for brain tumors: possible prediction of treatment response. *J Comput Assist Tomogr* 30, 496-500 (2006).

11. Leimgruber, A. *et al.* Perfusion and diffusion MRI of glioblastoma progression in a four-year prospective temozolomide clinical trial. *Int J Radiat Oncol Biol Phys* 64, 869-875, doi:10.1016/j.ijrobp.2005.08.015 (2006).

12. Balmaceda, C. *et al.* Multisection 1H magnetic resonance spectroscopic imaging assessment of glioma response to chemotherapy. *J Neurooncol* 76, 185-191, doi:10.1007/s11060-005-5261-2 (2006).

13. Ward, P. S. & Thompson, C. B. Metabolic reprogramming: a cancer hallmark even warburg did not anticipate. *Cancer Cell* 21, 297-308, doi:10.1016/j.ccr.2012.02.014 (2012).

14. Cairns, R. A., Harris, I. S. & Mak, T. W. Regulation of cancer cell metabolism. *Nat Rev Cancer* 11, 85-95, doi:10.1038/nrc2981 (2011).

15. Srinivas, P. R., Srivastava, S., Hanash, S. & Wright, G. L., Jr. Proteomics in early detection of cancer. *Clin Chem* 47, 1901-1911 (2001).

16. van Zijl, P. C. & Yadav, N. N. Chemical exchange saturation transfer (CEST): what is in a name and what isn't? *Magn Reson Med* 65, 927-948,

doi:10.1002/mrm.22761 (2011).

17. Zhou, J. Y., Payen, J. F., Wilson, D. A., Traystman, R. J. & van Zijl, P. C. M. Using the amide proton signals of intracellular proteins and peptides to detect pH effects in MRI. *Nat Med* 9, 1085-1090, doi:10.1038/nm907 (2003).

18. Zhou, J. Y. *et al.* Differentiation between glioma and radiation necrosis using molecular magnetic resonance imaging of endogenous proteins and peptides. *Nat Med* 17, 130-U308, doi:10.1038/nm.2268 (2011).

19. Togao, O. *et al.* Amide proton transfer imaging of adult diffuse gliomas: correlation with histopathological grades. *Neuro Oncol* 16, 441-448, doi:10.1093/neuonc/not158 (2014).

20. Sagiyama, K. *et al.* In vivo chemical exchange saturation transfer imaging allows early detection of a therapeutic response in glioblastoma. *Proc Natl Acad Sci U S A* 111, 4542-4547, doi:10.1073/pnas.1323855111 (2014).

21. Lazovic, J. *et al.* Nitroxoline induces apoptosis and slows glioma growth in vivo. *Neuro-Oncology* 17, 53-62, doi:10.1093/neuonc/nou139 (2015).

22. Zhou, J., Lal, B., Wilson, D. A., Laterra, J. & van Zijl, P. C. Amide proton transfer (APT) contrast for imaging of brain tumors. *Magn Reson Med* 50, 1120-1126, doi:10.1002/mrm.10651 (2003).

23. Hobbs, S. K. *et al.* Magnetic resonance image-guided proteomics of human glioblastoma multiforme. *J Magn Reson Imaging* 18, 530-536, doi:10.1002/jmri.10395 (2003).

24. Howe, F. A. *et al.* Metabolic profiles of human brain tumors using quantitative in vivo H-1 magnetic resonance spectroscopy. *Magnet Reson*

Med 49, 223-232, doi:10.1002/mrm.10367 (2003).

25. Tamai, K. *et al.* Diffusion-weighted MR imaging of uterine endometrial cancer. *J Magn Reson Imaging* 26, 682-687, doi:10.1002/jmri.20997 (2007).

26. Sunwoo, L. *et al.* Correlation of apparent diffusion coefficient values measured by diffusion MRI and MGMT promoter methylation semiquantitatively analyzed with MS-MLPA in patients with glioblastoma multiforme. *J Magn Reson Imaging* 37, 351-358, doi:10.1002/jmri.23838 (2013).

27. Surov, A., Meyer, H. J. & Wienke, A. Correlation Between Minimum Apparent Diffusion Coefficient (ADC(min)) and Tumor Cellularity: A Meta-analysis. *Anticancer Res* 37, 3807-3810, doi:10.21873/anticanres.11758 (2017).

28. Bharwani, N. *et al.* Diffusion-weighted imaging in the assessment of tumour grade in endometrial cancer. *Brit J Radiol* 84, 997-1004, doi:10.1259/bjr/14980811 (2011).

29. Yoshikawa, M. I. *et al.* Relation between cancer cellularity and apparent diffusion coefficient values using diffusion-weighted magnetic resonance imaging in breast cancer. *Radiat Med* 26, 222-226, doi:10.1007/s11604-007-0218-3 (2008).

30. Zhou, J. *et al.* Practical data acquisition method for human brain tumor amide proton transfer (APT) imaging. *Magn Reson Med* 60, 842-849, doi:10.1002/mrm.21712 (2008).

31. Oliva, C. R. *et al.* Acquisition of Temozolomide Chemoresistance in

Gliomas Leads to Remodeling of Mitochondrial Electron Transport Chain. *Journal of Biological Chemistry* 285, 39759-39767, doi:10.1074/jbc.M110.147504 (2010).

32. Clarke, M. J. *et al*. Effective sensitization of temozolomide by ABT-888 is lost with development of temozolomide resistance in glioblastoma xenograft lines. *Molecular Cancer Therapeutics* 8, 407-414, doi:10.1158/1535-7163.Mct-08-0854 (2009)

Figures

Figure 1.

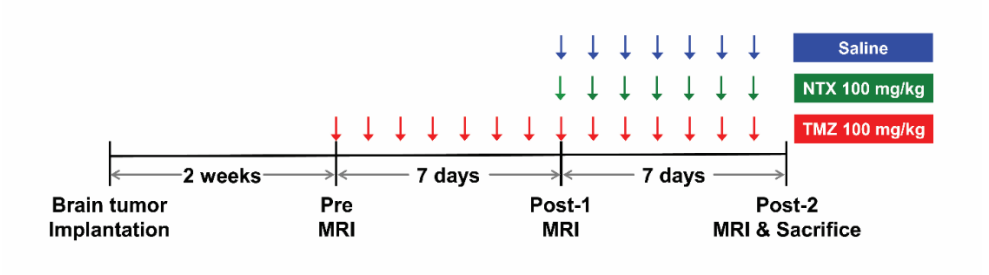

Experimental design for the *in vivo* study, showing the timeline of each group for LN229 cell inoculation, TMZ and NTX therapy, MR imaging, and animal sacrifice for brain harvest as described in the "Material and Methods" section.

Figure 2.

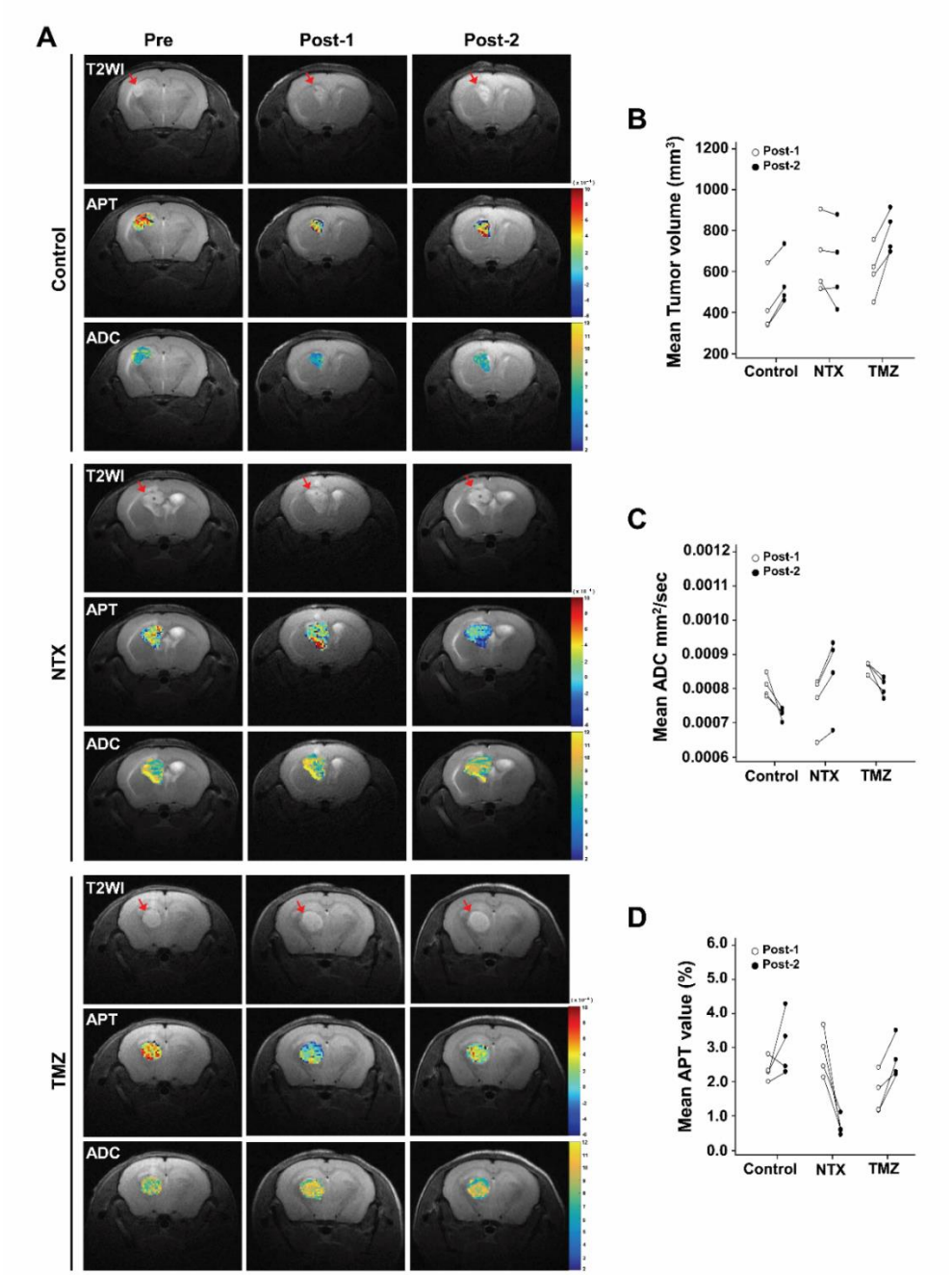

Comparison of the early evaluation of NTX-mediated therapeutic effects by APT and ADC (A) Representative T2WIs (1st row), APT maps (2nd row) and ADC (3rd

row) for control group, T2WIs (4th row), APT maps (5th row) and ADC maps (6th row) for NTX group, and T2WIs (7th row), APT maps (8th row) and ADC maps (9th row) for TMZ group, imaged on pretreatment MRI, post-1 and post-2 MRI. (B) The tumor volume decreased on post-2 MRI in NTX-treated mice (P = 0.6857) without statistical significance, and the control (P = 0.2000) and TMZ groups showed an increase in tumor volume without statistical significance (P = 0.1143). (C) The ADC (mm2/sec) value increased on the post-2 MRI after NTX treatment without statistical significance (P = 0.2000). However, control group (P = 0.0286) and TMZ-treated mice (P = 0.0286) showed a significant decrease in ADC value. (D) The APT value (%) was significantly decreased after NTX treatment (P = 0.0286). However, the APT value was not significantly decreased in the control group (P = 0.3429) and TMZ-treated mice (P = 0.1143). Data are represented as median with an interquartile range of four independent mice in each group.

Figure 3.

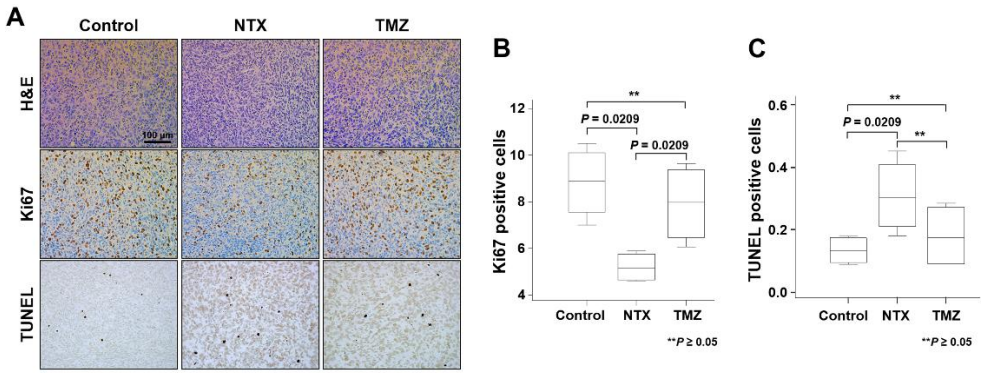

Quantification of immunohistochemistry studies. (A) Histological images representing hematoxylin and eosin staining for the morphology of tumor (1st row), immunohistochemistry images of Ki67 for cellular proliferation (2nd row), and TUNEL staining for DNA damage (3rd row) for control, NTX, and TMZ group, respectively. Scale bar is 100 µm in X 200. (B) Significantly decreased expression of Ki67 reflects the decreased cell proliferation in NTX-treated animals (P = 0.0209) compared with the control. The Ki67 expression was significantly increased in TMZ-treated mice (P = 0.0209) compared to that in NTX-treated mice. No significant difference was observed between control and TMZ-treated mice. (C) Significantly increased TUNEL positive cells reflects the increased DNA damage in NTX-treated animals (P = 0.0209) compared with that in the control animals. No significant changes in DNA damage were observed between untreated and TMZ-treated mice (P = 0.5637) or NTX- and TMZ-treated mice (P = 0.2482). Data are represented as median with an interquartile range of four independent experiments.

Figure 4.

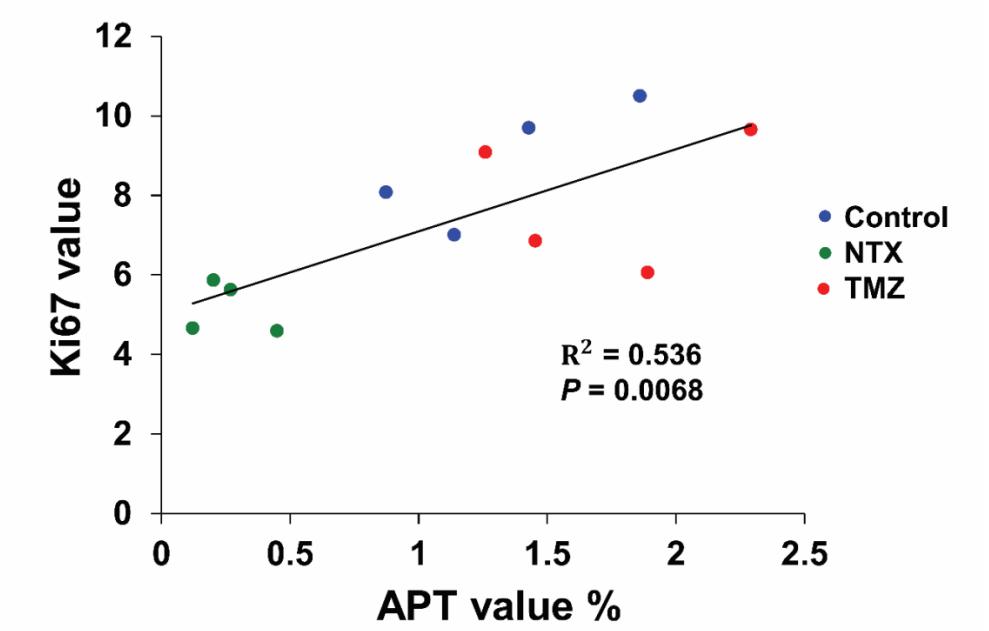

Correlation between the APT and Ki67 labeling index. Ki67 showed a positive correlation (R^2 = 0.536) (P = 0.0068) (n = 4 per group) with the APT value in all experimental groups.

국문 초록

Amide proton Transfer 영상을 이용한 Temozolomide 내성 교모세포종에서의 Nitroxoline 조기 치료 반응 평가: 확산강조영상과의 비교

서울대학교 대학원
협동과정 종양생물학전공
니샨 타쿠르 (Nishant Thakur)

목적: Amide proton transfer (APT) 영상 (아마이드 수소 이동 영상기법)은 화학적 포화 전달 교환을 통한 내인성 이동 단백질과 펩타이드를 검출하는 새로운 분자 MRI 기술이다. 이 연구의 목적은 temozolomide (TMZ, 테모졸로마이드) 내성을 지닌 교모세포종 마우스 모델에서 nitroxoline (NTX, 나이트록솔린)에 대한 조기 치료 반응 모니터링 시, APT 영상의 반응 평가 예측능을 확산강조영상과 비교하여 평가하는 것이다.

방법: 본 연구는 서울대학교병원의 동물용 의약품 사용위원회의 승인을 받았다. TMZ 내성 교모세포종 마우스 모델 (n = 12)을 7일동안 100mg/kg/d의 NTX (n = 4), TMZ (n = 4), 혹은 생리 식염수 (n = 4)로 단기간 처리를 한 뒤, APT 영상 및 확산강조영상을 이용하여 순차적으로 사용하여 평가하였다. APT 신호 강도 및 겉보기 확산 계수 (ADC) 값을 계산하고 약물 처리 전후를 비교하였다. 면역 조직학적 분석을 통해 APT 이미징과 조직 병리학 사이의 상관 관계를 분석하였다. APT 값과 Ki67 라벨링 지수 사이의 연관성은 단순선형회귀분석을 사용하여 평가하였다.

결과:

우리는 단기 NTX 치료 이후의 종양 크기의 감소를 관찰하였고 (P = 0.6857), 대조군 (P = 0.2000) 과 TMZ군 (P = 0.1143) 에서는 종양 크기의 증가를 관찰하였다. 그리고 단기 NTX 처리는 처리하지 않은 그룹 (P = 0.3429) 과 TMZ 그룹 (P = 0.1143) 에 비해 APT 값이 통계적으로 유의하게 감소하였다 (P = 0.0286). 하지만, 단기 NTX 처리 후의 ADC 값의 유의한 증가는 관찰할 수 없었다 (P = 0.2000). 반면에 NTX 처리하지 않은 그룹 (P = 0.0286) 과 TMZ를 처리 (P= 0.0286) 한 마우스에서 ADC값은 유의 하게 감소하였다. 게다가 우리의 조직학적 자료는 NTX 처리 그룹에서 처리하지 않은 마우스에 비해 Ki67의 발현량이 낮았다. 또한 Ki67 라벨링 지수는 APT 값과의 상관관계를 보여준다.

결론: APT 영상은 TMZ 저항성 마우스 모델에서 ADC 값과 비교하여 NTX 치료에 대한 초기 반응을 확인하는데 있어 더 도움이 됨을 확인하였다. 본 연구를 통해 APT 영상 기법이 교모세포종 환자의 조기 치료 평가를 위한 유용한 이미징 바이오 마커가 될 것으로 기대한다.

.....

주요어: 아미드 수소 영상, 겉보기 확산 계수, 화학 교환 포화 전달 영상, 나이트록솔린, 테모졸로마이드 내성을 지닌 교모세포종 마우스 모델

학 번: 2016-24265

Acknowledgement

Foremost, I would like to express my sincere gratitude to my advisors Professor Seung Hong Choi and Professor Hye Rim Cho for their continuous support, patience, guidance, motivation and immense knowledge during my master study and research. Their guidance helped me all the time of research and writing of this thesis.

Besides my advisor, I would like to thank the rest of my thesis committee: Professor Ii Han kim and Professor Chul Ho Sohn for their encouragement, comments, and questions. I would also express my gratitude toward Professor Sung Joon Kim for provided me extra classes of Human Physiology.

My sincere thanks to Nisha Kumari for guiding me in my research. Due to her guidance and efforts that I could finish my Master requirement.

I thank my lab mates in Molecular and Neuroimaging Translational lab: Hyejin Jeon, Vu Thi Hien and Yong Sub Shin for helped me the direct and indirect way. I also thank my friends in Himachal Pradesh University (India): Kishori Garg, Lalit Sagar, Sunil Katwal, Pankaj Rana, Nitin Thakur and Vinod Kumar for their motivation.

Apart from my lab member, I would like to thank my Korean Friends Sanghyeon Lee, Jae Man Song and Sunha Park for helping me in the translation of my English abstract into Korean abstract.

I also thank Dr. Shashi Bhatia, Dr. Jaywant Gunjakar, Dr. Santosh Kumar, Dr. Raj Kumar Patel, Prashant Sharma, Vinay Kumar and Nadeem Ahmed Lodi for their guidance and support.

Last but not the least, I would like to thank my family: father Dalip Singh, mother Venna Devi, uncle Ashok Datyal, aunt Raj kumari, brother in law Dr. Manu Kumar, brother Prashant Thakur, sister Sapna Kumari, Smita Thakur, grandfather Ram Krishan, grandmother Kausalya Devi and my extended family for their help and encouragement.

Nishant Thakur

CURRICULUM VITAE

Nishant Thakur

EDUCATION

08/2016 – 02/2019	College of Medicine, Seoul National University, Master in Interdisciplinary Program in Cancer Biology. Researcher in Molecular and Translation laboratory and Institute for Basic Science (IBS).
06/2014 – 07 /2015	Himachal Pradesh University Summer Hill, Bachelor of Education.
06/2011 - 05/2014	Himachal Pradesh University Summer Hill, Bachelor of Science.

PUBLICATIONS

1. Nisha Kumari, **Nishant Thakur** (*co-first author*), Hye Rim Cho, Seung Hong Choi. **"Assessment of Early Therapeutics Response to Nitroxoline in Temozolomide Resistant Glioblastoma by Amide Proton Transfer Imaging: A Comparative Study with Diffusion-weighted Imaging**" (Submitted in Scientific Report).

2. Hye Rim Cho, Nisha Thakur, **Nishant Thakur**, Seung Hong Choi. "**Nitroxoline Exhibit Anticancer Activity Inducing Apoptosis in A Temozolomide-resistant Glioblastoma**" (Submitted in Neoplasia).

PRESENTATION

1. Nishant Thakur, Nisha Kumari, Hyejin Jeon, Jooyeon Chung, Hye Rim Cho, Seung Hong Choi. **"Comparison of CEST and DWI MRI to Evaluate Early Response of Nitroxoline Treatment in Temozolomide-resistant Glioblastoma Model**". 22nd Annual Scientific Meeting and Education day of the Society for Neuro-Oncology was held at San- Francisco on Nov 16-19, 2017 (Poster Presentation).

2. Nishant Thakur, Nisha Kumari, Hyejin Jeon, Jooyeon Chung, Hye Rim Cho, Seung Hong Choi. **"Comparison of CEST and DWI MRI to Evaluate Early Response of Nitroxoline Treatment in Temozolomide-resistant Glioblastoma Model**". 22nd International Congress on Magnetic Resonance Imaging/Korean Society of Magnetic resonance in Medicine was held at Seoul on March 29-31, 2018 (Oral Presentation).

HONOR

Best Oral Presentation Award

2018 International Congress of Magnetic Resonance Imaging/Korean Society of Magnetic resonance in Medicine.